Modelling self-sensing of a magnetostrictive actuator based on a terfenol-D rod*

Yan Bai-Ping(严柏平)[a)†], Zhang Cheng-Ming(张成明)[b)], Li Li-Yi(李立毅)[b)], Tang Zhi-Feng(唐志峰)[a)], Lü Fu-Zai(吕福在)[a)], and Yang Ke-Ji(杨克己)[a)]

[a)] *Institute of Modern Manufacturing Technology, Zhejiang University, Hangzhou* 310058, *China*

[b)] *School of Electrical Engineering and Automation, Harbin Institute of Technology, Harbin* 150001, *China*

(Received 4 June 2014; revised manuscript received 16 July 2014; published online 10 October 2014)

A simplified quasi-static computational model for self-sensing applications of magnetostrictive actuators based on terfenol-D rods is presented. Paths and angle changes in the magnetic moments rotation of $Tb_{0.3}Dy_{0.7}Fe_2$ alloy are studied as functions of compressive stress and magnetic field, and then used to determine the magnetization in its actuation. Then sensing of magnetic induction picked from a driving coil in an actuator is derived. The model is quick and efficient to solve moments rotation and its magnetization. Sensing results of compressive stress and magnetostriction calculated by the model are in good agreement with experiments and will be helpful in the design and control of self-sensing applications in actuators.

Keywords: self-sensing model, magnetostrictive actuator, $Tb_{0.3}Dy_{0.7}Fe_2$ alloy, moments rotation

PACS: 75.80.+q, 75.60.–d, 75.60.Ej **DOI:** 10.1088/1674-1056/23/12/127504

1. Introduction

Magnetostrictive actuators based on $Tb_{0.3}Dy_{0.7}Fe_2$ alloy (called terfenol-D) have extensive application prospects in many fields for their favorable mechanical properties, such as precision positioning systems, vibration controlling systems, and flow control (like pumps and valves).[1,2] In the applications of actuators, improving the repeatability and accuracy of magnetostriction has received much attention. Most researchers have used independent sensors to make actuators work in close-loop feedback systems,[3,4] but excessive sensors are needed to design and control the actuator, which is not suitable for micro integrated applications.

A self-sensing actuator based on $Tb_{0.3}Dy_{0.7}Fe_2$ alloy has both driving and sensing functions and can sense the changes in the magnetization and magnetostriction of an alloy in its actuation. Due to the absence of a suitable model, the application of a self-sensing actuator based on magnetostrictive material is still under development. The simplest self-sensing model is the one in which magnetostriction is calculated by linear piezomagnetic equations.[5–7] While this is quick to implement, it cannot incorporate nonlinear effects and is limited to use in an area of small linear effects. Based on the Stoner–Wohlfarth (SW) model, researchers[8–15] have investigated the nonlinear magnetomechanical effect and magnetostriction in $Tb_{0.3}Dy_{0.7}Fe_2$ alloy through calculating magnetic moment rotation and its fractional changes. Much has been learned, but the procedure of free energy minimization is complex, and solving the minimum via moments rotation in three dimensions is computation-intensive, so it is difficult to employ in constructing a self-sensing model for actuator applications. So far, there is still no report about an actual application of a self-sensing actuator based on a terfenol-D rod.

In this paper, a simplified computational model for the self-sensing application of magnetostrictive actuators is presented. On the basis of the SW model, the free energy minimization procedure of magnetic moments rotation is simplified, using coordinate transformation and a graphical solution technique. The paths and angle changes of moment rotation in the $Tb_{0.3}Dy_{0.7}Fe_2$ alloy are investigated with compressive stress and field, and then used to model magnetization sensing in an actuator. Lastly, an actuator is designed and an experimental test bench is set up to verify the validity of the sensing model in its actuation.

2. Model development

2.1. Domains rotation in $Tb_{0.3}Dy_{0.7}Fe_2$ alloy

To investigate the rotation of moments in single crystal $Tb_{0.3}Dy_{0.7}Fe_2$ alloy with varying compressive stress and magnetic fields, the free energy formulation given by the SW model[16,17] is used. The magnetization of the [110] aligned $Tb_{0.3}Dy_{0.7}Fe_2$ alloy consisting of noninteracting single-domain particles can be solved by the minimum energy of the particles, and the free energy per unit of the domain particle can be written as

$$E = K_1(\alpha_1^2\alpha_2^2 + \alpha_2^2\alpha_3^2 + \alpha_1^2\alpha_3^2) + K_2(\alpha_1^2\alpha_2^2\alpha_3^2)$$

*Project supported by the National Preeminent Youth Foundation (Grant No. 51225702) and the National Natural Science Foundation of China (Grant No. 51177024).

†Corresponding author. E-mail: d_enip@163.com

© 2014 Chinese Physical Society and IOP Publishing Ltd

$$-\frac{3}{2}\lambda_{100}\sigma(\alpha_1^2\beta_1^2+\alpha_2^2\beta_2^2+\alpha_3^2\beta_3^2)$$
$$-3\lambda_{111}\sigma(\alpha_1\alpha_2\beta_1\beta_2+\alpha_2\alpha_3\beta_2\beta_3+\alpha_1\alpha_3\beta_1\beta_3)$$
$$-\mu_0 M_s H_e(\alpha_1\gamma_1+\alpha_2\gamma_2+\alpha_3\gamma_3), \quad (1)$$

where α_1, α_2, α_3 are direction cosines of magnetization M; β_1, β_2, β_3 are direction cosines of compressive stress σ; and γ_1, γ_2, γ_3 are direction cosines of magnetic field H. In a terfenol-D rod, the compressive stress and magnetic field have the same direction, along the [110] axes in the alloy, so direction cosines $\beta_i=\gamma_i$. K_1 and K_2 are the magnetocrystalline anisotropy constants, λ_{100} and λ_{111} are saturation magnetostriction coefficients of the $\langle 100\rangle$ and $\langle 111\rangle$ axes, M_s is the saturation magnetization.

It has been shown in Eq. (1) that the free energy is a three-dimensional case of direction cosines α_i, the procedure of direction cosines α_i solved by the minimum energy of moment is complex, and computing the minimum via moments rotation is computation-intensive.

Coordinate transformation and a graphical solution technique are used in this paper to simplify the minimization solutions. The angle θ between magnetic field H and magnetization M can be analyzed as a function of α_i, expressed as $\theta(\alpha_i)$, so the rotation of domains and its magnetization in alloy can be described by the changes of angle θ. To calculate angle θ, new coordinates $Y(x_1, y_1, z_1)$ are set, which use the [110] direction as the z_1 axis, and the x_1 and y_1 axes lie in the (110) plane. Then magnetization M can be expressed as (M, θ, ϕ) in the Y coordinates, where ϕ is the angle of magnetization in the x_1–y_1 plane. The coordinate transformation relation from X ([100], [010], [001] axes) into Y coordinates can be given as

$$Y^{\mathrm{T}}(1,\theta,\phi) = \begin{bmatrix} x_{11} & x_{12} & x_{13} \\ x_{21} & x_{22} & x_{23} \\ x_{31} & x_{32} & x_{33} \end{bmatrix} \cdot X^{\mathrm{T}}(\alpha_1,\alpha_2,\alpha_3)$$
$$= x_{ii}\cdot X^{\mathrm{T}}(\alpha_1,\alpha_2,\alpha_3), \quad (2)$$

where

$$x_u = \begin{bmatrix} 1/2 & -1/2 & -\sqrt{2}/2 \\ -1/2 & 1/2 & -\sqrt{2}/2 \\ \sqrt{2}/2 & \sqrt{2}/2 & 0 \end{bmatrix}$$

is used in this paper. Taking Eq. (2) into Eq. (1), the free energy will be simplified to a two-dimensional equation of angles θ and φ, expressed as $E(\theta,\varphi)$, and the rotation of magnetic domains can be solved by plotting free energy equipotential curves as functions of angle θ and φ in Fig. 1. It has been shown in Fig. 1 that the domain angle is distributed in eight $\langle 111\rangle$ axes with no compression, where [111] $[11\bar{1}]$ $[\bar{1}\bar{1}1]$ $[\bar{1}\bar{1}\bar{1}]$ are arranged in plane $(\bar{1}10)$ and $[\bar{1}11]$ $[1\bar{1}1]$ $[1\bar{1}\bar{1}]$ $[\bar{1}1\bar{1}]$ lie within the (110) plane. Reversibility and irreversibility are both contained in the domains rotation process with the compression increasing (red color path in Fig. 1), and irreversible domain rotation occurs at the critical compressive stress σ_s, which causes a sudden transition of angle θ, called the jump effect of moment rotation. Continuous domains rotation occurs in both plane $\varphi=\varphi_0$ ($\bar{1}10$ plane) and $\theta=90^\circ$ ((110) plane) in a reversible process, where φ_0 is the original domain angle with 0-MPa compression, and discontinuous rotation occurs at the critical compressive stress, leading to domains jumping from the plane into the (110) plane. Also, by using this analysis method, it is easy to show that domain rotation occurs in the $\varphi=\varphi_i$ plane in the action of a magnetic field, where φ_i is the angle with compressive stress σ.

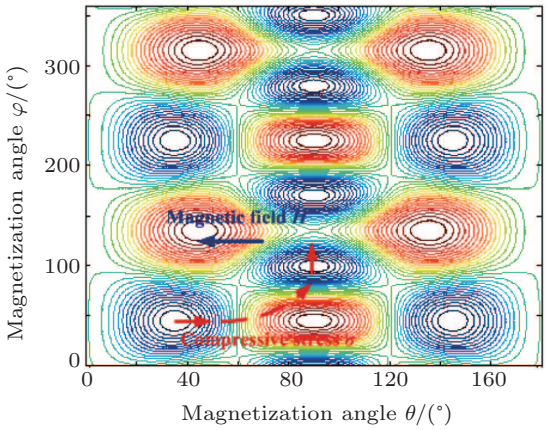


Fig. 1. (color online) Equipotential curves of free energy as a function of angle θ and φ with 0 MPa compression plotted by Eqs. (1) and (2). Paths of the domain rotation introduced with compressive stress σ (red color) and magnetic field H (blue color).

The rotation and jump effects of magnetic moments can be expressed clearly by the continuous and discontinuous paths of $[11\bar{1}]$ ($\theta_0=35.3^\circ$, $\varphi_0=45^\circ$) oriented domains. The magnetostriction of the $[11\bar{1}]$-oriented domain with compressive stress and magnetic fields have two different rotation paths, continuous rotation just in the $(\bar{1}10)$ plane ($\sigma<\sigma_s$) and the $(\bar{1}10)$ plane ($\varphi=\varphi_0$ plane) $\rightarrow$ (110) plane ($\theta=90^\circ$ plane) $\rightarrow$ $\varphi=\varphi_i$ plane rotation ($\sigma\geq\sigma_s$) see in Fig. 1. The rotations occurring within the $(\bar{1}10)$, (110), and $\varphi=\varphi_i$ planes are reversible, and their free energy can be simplified as

$$E_{(\bar{1}10)} = K_1\left(\frac{1}{4}\cos^4\theta+\sin^2\theta\cdot\cos^2\theta\right)+\frac{K_2}{4}\sin^2\theta\cdot\cos^4\theta$$
$$-\frac{3}{4}\sigma\cos^2\theta\cdot(\lambda_{100}+\lambda_{111})-\mu_0 M_s H_e\cos\theta, \quad (3)$$
$$E_{(110)} = K_1\left(\frac{1}{4}\cos^4(\varphi-135)\right.$$
$$\left.+\sin^2(\varphi-135)\cdot\cos^2(\varphi-135)\right)$$
$$+\frac{K_2}{4}\sin^2(\varphi-135)\cdot\cos^4(\varphi-135)$$
$$-\frac{3}{4}\sigma\cos^2(\varphi-135)\cdot(\lambda_{100}-\lambda_{111}). \quad (4)$$
$$E_{\varphi=\varphi_i} = E(\theta,\varphi_i). \quad (5)$$

To solve the critical compressive stress σ_s and magnetization angle θ, the energy equation (3) is plotted as a function of angle θ with various compressive stress in Fig. 2. The $[11\bar{1}]$-oriented direction of magnetization is initially $\theta = 35.3^\circ$ at 0-MPa compression, where a stable energy minimum occurs. Increasing compression translates this minimum reversibly until a critical compressive stress σ_s is reached, which can be obtained from the constraint condition of the inequality $E(\theta_i, \varphi_0) < E(\theta_i, \varphi_0 + \varphi)$. In the φ region of (θ_i, φ_0), θ_i is the energy minimum angle under compression. It has been shown in Fig. 2 that $E(\theta_i, \varphi_0) < E(\theta_i, \varphi_0 + \varphi)$ occurs at $\sigma < \sigma_s$ and $E(\theta_i, \varphi_0) \geq E(\theta_i, \varphi_0 + \varphi)$ at $\sigma \geq \sigma_s$, so a stable energy minimum can be found by plotting energy curves with the constraint condition $E(\theta_i, \varphi_0) < E(\theta_i, \varphi_0 + \varphi)$, and then the $[11\bar{1}]$-oriented domain jumps into the (110) plane, so it can be solved by Eqs. (4) and (5).

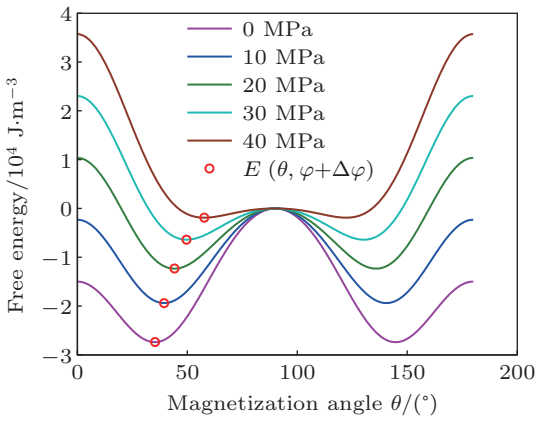


Fig. 2. (color online) Energy curves of $[11\bar{1}]$-oriented domain in the $(\bar{1}10)$ plane with increasing compressive stress. The constraint condition of inequality $E(\theta_i, \varphi_0) < E(\theta_i, \varphi_0 + \varphi)$ is used to solve the stable energy minimum and critical compressive stress σ_s.

2.2. Magnetization calculation of domains rotation

So, the paths of domains rotation can be calculated through plotting free energy $E(\theta, \varphi)$. Equipotential curves, the magnetization angle (θ, φ), and critical compressive stress σ_s can be solved by Eqs. (3)–(5). Those continuous and discontinuous rotations in alloy lead to the changes in the fractional occupancy of the eight $\langle 111 \rangle$-oriented domains.[18,19] The total magnetization and magnetostriction of magnetostrictive materials can be calculated by the magnetization angle (θ, φ) and the fractional occupancy, which can be written as

$$M = \sum_{j=1}^{8} V_j \cdot M_s \cos\theta_j, \tag{6}$$

$$V_j = \frac{K \exp(-E_j/\omega)}{\sum_{i=1}^{8} K \exp(-E_j/\omega)}, \tag{7}$$

$$\lambda = k \sum_{j=1}^{8} V_j \cdot \left\{ \frac{3}{2} \cdot \lambda_{100} (\alpha_1^2 \beta_1^2 + \alpha_2^2 \beta_2^2 + \alpha_3^2 \beta_3^2) + 3\lambda_{111} (\alpha_1 \alpha_2 \beta_1 \beta_2 + \alpha_2 \alpha_3 \beta_2 \beta_3 + \alpha_1 \alpha_3 \beta_1 \beta_3) \right\}, \tag{8}$$

where j indexes the domains along the eight $\langle 111 \rangle$ axes, θ_j is the magnetization angle of the domain and V_j is the fractional occupancy of a j domain particle, k is the correction coefficient of magnetostriction, K is a normalization factor, and ω is the potential distribution parameter. Based on Refs. [20]–[22] and experimental behaviors of magnetostrictive materials, properties of terfenol-D in this paper are given as $k\lambda_{111} = 1273$ ppm, $K_1 = -6 \times 10^4$ J/m^3, $K_2 = -3.4 \times 10^5$ J/m^3, $M_s = 7.65 \times 10^5$ A/m, $\omega = 10^4$. The solutions of magnetization can be numerically obtained from Eqs. (3)–(7) with the rotation paths of the domain; see results in Fig. 3. Compared to experiments with varying compressions and fields, modeling results are in a good agreement with the experiments.

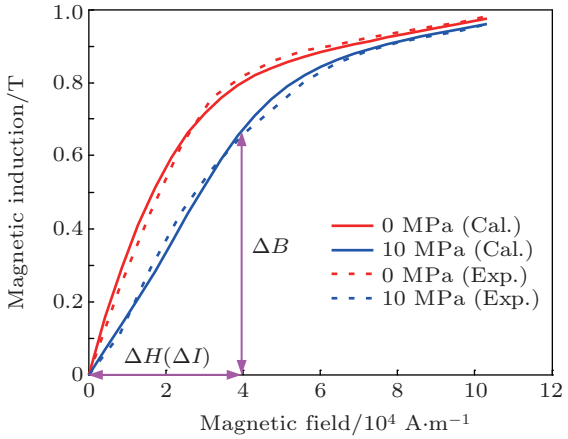


Fig. 3. (color online) Comparison between calculated and experimental results of the total magnetic induction for a terfenol-D rod as a function of the magnetic field.

2.3. Sensing model of actuators

In applications of magnetostrictive actuators, the changes in magnetic induction B with driving current I can be calculated from voltage U–current I signal of a driving coil, used to sense compressive stress on the terfenol-D rod. Based on the sensing results of compressive stress, magnetostriction of the actuator can be obtained by Eq. (8). Figure 4(a) is a typical structure of an actuator driven by a terfenol-D rod, fixed in the middle of the actuator by an external nylon framework. A solenoid coil, driven by an external current supply, is used to provide the magnetic field, and the external magnetic field circuit is made of a high-permeability material. Besides being used to make the driving field, the current coil can also be used to sense magnetization changes of the terfenol-D rod in the actuator. The voltage U–current I relation in the driving coil can be given as

$$U = RI + \frac{\Delta\psi}{\Delta t} = RI + \frac{NS_{\mathrm{GMM}}\Delta B_{\mathrm{GMM}} + \mu_0 N^2 / l_0 S_{\mathrm{nylon}} \Delta I + \Delta\psi_{\mathrm{coil}}}{\Delta t}, \tag{9}$$

where R is the resistance of the coil, t is the action time of the field changes, and Ψ is the magnetic flux change in the coil, including flux change in the terfenol-D rod, the nylon and the coil, where N is the turns of the coil, $S_{\rm GMM}$ and $S_{\rm nylon}$ are the cross sectional areas of GMM and nylon, $B_{\rm GMM}$ is changes of magnetic induction induced by driving current I, l_0 is the length of the terfenol-D rod, Ψ is the flux change in the coil area, can be calculated as

$$\Delta\psi_{\rm coil} = \int_{R_1}^{R_2}\int_{R_1}^{a} \frac{\mu_0 N^2/l_0}{(R_2-R_1)^2}(R_2-r)2\pi r{\rm d}r\cdot{\rm d}a\cdot\Delta I, \quad (10)$$

where R_1 and R_2 are the inner and outer radii of the coil. With reference to Eqs. (6)–(8), the sensing change of magnetization in the coil can be expressed as

$$\Delta B_{\rm GMM} = \frac{\int(U-RI){\rm d}t - \mu_0 N^2(S_{\rm nylon}+S^*_{\rm coil})/l_0\cdot\Delta I}{NS_{\rm GMM}}. \quad (11)$$

In Eq. (11),

$$S^*_{\rm coil} = \int_{R_1}^{R_2}\int_{R_1}^{a}\frac{2\pi}{(R_2-R_1)^2}(R_2-r)r{\rm d}r\cdot{\rm d}a$$

is the equivalent area of the sensing coil with a uniformity field. In an actuator, we can monitor the U–I relation to sense magnetic induction changes in magnetostrictive material. On the basis of these results, the compression and magnetostriction of the actuator can be calculated by Eqs. (3)–(8).

3. Comparison with experimental data

In this paper, a small giant magnetostrictive actuator is designed and an experimental test bench (Fig. 4) is set up to confirm the validity of our sensing model. The turns of the driving solenoid coil $N = 688$, and the dimension is set to be ϕ22 mm×ϕ10 mm×43 mm.

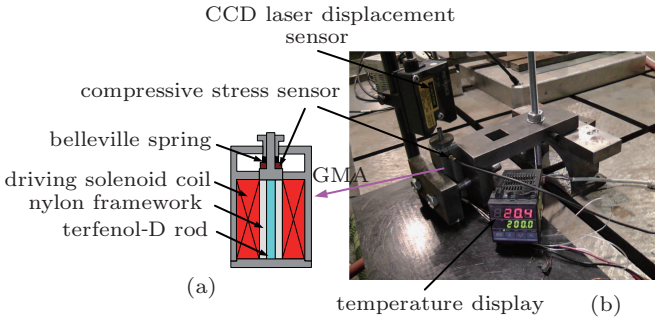


Fig. 4. (color online) Schematic structure and test bench photo of a giant magnetostrictive actuator based on a terfenol-D rod. Magnetostriction is measured by a CCD laser displacement sensor. A temperature display is used to monitor the changes of temperature in the actuator. Panel (a) is the structure of the actuator; panel (b) is the test bench for actuator.

The back-EMF signal can be calculated from the U–I relation, and pulse input current is used in this paper. Figure 5 shows the results of the electrical signal picked up by the driving current coil in the experiment. Combining Eq. (11) with Eqs. (3)–(8), sensing results of compressive stress and magnetostriction can be obtained; see Fig. 6.

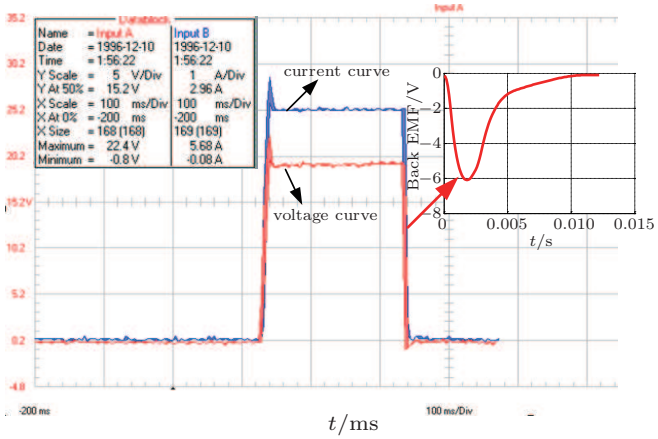


Fig. 5. (color online) Experimental test of U–I curves and back-EMF. The back-EMF signal is calculated on the trailing edge of the U–I pulse.

Sensing experimental results of the actuator are shown in Fig. 6. Figure 6(a) shows the sensing results of compressive stress in the actuator, which is in good agreement with the experimental data, especially in the 1-A∼3-A current (17.2 kA/m–51.6 kA/m field); the max error of the compressive stress sensing result can be kept within 1 MPa.

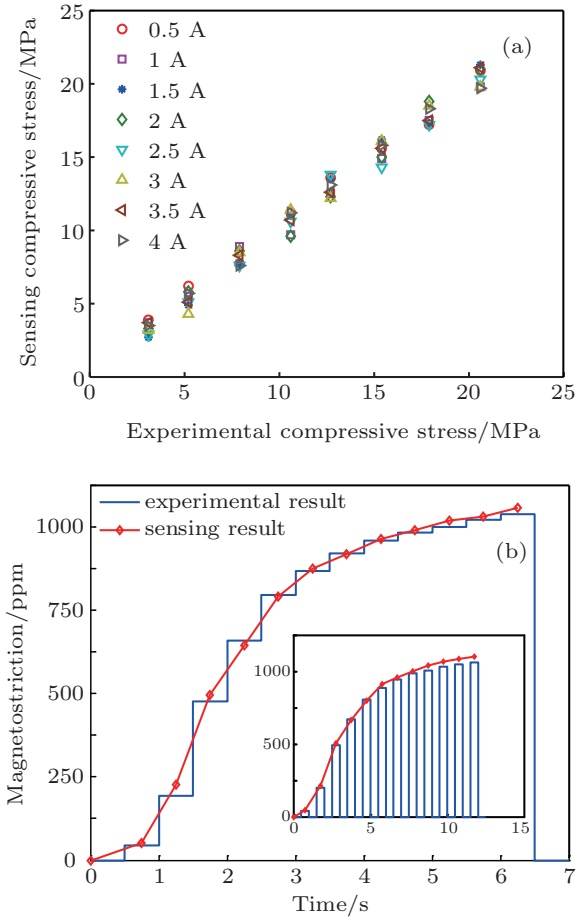


Fig. 6. (color online) Comparison between the experimental and sensing results of the magnetostrictive actuator based on a terfenol-D rod: (a) compressive stress results with varied driving current; (b) magnetostriction results with single-pulse and continuous-pulse driving current (current increment of each pulse is 0.5 A).

Based on the sensing results of compression, the magnetostriction of the actuator under two types of driving current (current increment of each pulse is 0.5 A), single-pulse current, and continuous-pulse current, is calculated in Fig. 6. The maximum sensing error of magnetostriction is just 62.5 ppm (2.5 μm), and the results indicate that single-pulse sensing has good results with a low current ($I \leq 3.5$ A), and high-current sensing has good applicability in continuous current.

4. Conclusion

This paper presents a simplified quasi-static computational model applied to the self-sensing application of a magnetostrictive actuator based on a terfenol-D rod. Calculations by the model are in good agreement with experimental results, especially in low magnetic field. The model can be quick and efficient when used to sense compressive stress and magnetostriction in actuator applications. The results will also be helpful for the design and control of self-sensing applications of actuators.

References

[1] Grunwald A and Olabi A G 2008 *Sens. Actuators A* **144** 161

[2] Karunanidhi S and Singaperumal M 2010 *Sens. Actuators A* **157** 185

[3] Tang Z F, Lü F Z and Xiang Z Q 2008 *J. Zhejiang Univ. Sci. A* **9** 99

[4] Jon P and Alison B F 1995 *J. Int. Mater. Syst. Struct.* **6** 639

[5] Kuhnen K, Schommer M and Janocha H 2007 *Smart Mater. Struct.* **16** 1098

[6] Clephas B and Janocha H 1998 *Proc. SPIE* **3329** 174

[7] Bottauscio O, Roccato P E and Zucca M 2010 *IEEE Trans. Magn.* **8** 46

[8] Jiles D C and Hariharan S 1990 *J. Appl. Phys.* **67** 5013

[9] Zhang H 2011 *Appl. Phys. Lett.* **98** 232505

[10] Wang Z B, Liu J H and Jiang C B 2010 *Chin. Phys. B* **19** 117504

[11] Zhang H and Zeng D C 2010 *Acta Phys. Sin.* **59** 2808 (in Chinese)

[12] Zheng L, Jiang C B, Shang J X and Xu H B 2009 *Chin. Phys. B* **18** 1647

[13] Li L Y, Yan B P, Zhang C M and Cao J W 2012 *Acta Phys. Sin.* **61** 167506 (in Chinese)

[14] Zhang C S, Ma T Y, Pan X W and Yan M 2012 *Chin. Phys. Lett.* **29** 027501

[15] Jiang C B, Zhou S Z and Wang R 1998 *Chin. Phys. Lett.* **15** 379

[16] Armstrong W D. 2002 *J. Appl. Phys.* **91** 2202

[17] Mei W, Okane T and Umda T 1998 *J. Appl. Phys.* **84** 6208

[18] Zhang H, Zeng D C and Liu Z W 2011 *Acta Phys. Sin.* **60** 067503 (in Chinese)

[19] Jin Y M and Chopra H D 2011 *Phys. Rev. B* **84** 140401

[20] Zhang C S, Sun G G, Yan M and Ma T Y 2014 *Appl. Phys. Lett.* **104** 052409

[21] Yang Y V, Huang Y Y and Jin Y M 2011 *Appl. Phys. Lett.* **98** 012503

[22] Hu C C, Shi Y G, Shi D N, Tang S L, Fan J Y and Du Y W 2013 *J. Appl. Phys.* **113** 203906